Molecular Biology of the Cell
Vol. 21, 1763–1771, May 15, 2010

Mitf Induction by RANKL Is Critical for Osteoclastogenesis

Ssu-Yi Lu, Mengtao Li, and Yi-Ling Lin

Section of Oral Pathology, Department of Diagnostic and Surgical Sciences, School of Dentistry, University of California, Los Angeles, CA 90095

Submitted July 20, 2009; Revised March 1, 2010; Accepted March 18, 2010
Monitoring Editor: Marianne Bronner-Fraser

Microphthalmia-associated transcription factor (Mitf) regulates the development and function of several cell lineages, including osteoclasts. In this report, we identified a novel mechanism by which RANKL regulates osteoclastogenesis via induction of Mitf isoform E (Mitf-E). Both Mitf-A and Mitf-E are abundantly present in osteoclasts. Unlike Mitf-A, which is ubiquitously expressed and is present in similar amounts in macrophages and osteoclasts, Mitf-E is almost nondetectable in macrophages, but its expression is significantly up-regulated during osteoclastogenesis. In addition to their different expression profiles, the two isoforms are drastically different in their abilities to support osteoclastogenesis, despite sharing all known functional domains. Unlike Mitf-A, small amounts of Mitf-E are present in nuclear lysates unless chromatin is digested/sheared during the extraction. Based on these data, we propose a model in which Mitf-E is induced during osteoclastogenesis and is closely associated with chromatin to facilitate its interaction with target promoters; therefore, Mitf-E has a stronger osteoclastogenic activity. Mitf-A is a weaker osteoclastogenic factor, but activated Mitf-A alone is not sufficient to fully support osteoclastogenesis. Therefore, this receptor activator for nuclear factor-κB ligand (RANKL)-induced Mitf phenomenon seems to play an important role during osteoclastogenesis. Although the current theory indicates that Mitf and its binding partner Tfe3 are completely redundant in osteoclasts, using RNA interference, we demonstrated that Mitf has a distinct role from Tfe3. This study provides the first evidence that RANKL-induced Mitf is critical for osteoclastogenesis and Mitf is not completely redundant with Tfe3.

INTRODUCTION

During normal physiological conditions, osteoclast differentiation is regulated by osteoblasts and stromal cells, both of which provide two essential osteoclastogenic factors, macrophage–colony-stimulating factor (M-CSF) and receptor activator of nuclear factor (NF)-κB ligand (RANKL), along with a number of other positive and negative regulatory factors. The primary role of M-CSF is to provide survival signals during osteoclastogenesis (Lagasse and Weissman, 1997). In contrast, RANKL provides osteoclast-specific differentiation signals and activates multiple signal transduction pathways, which turn on transcription factors NF-κB, c-Fos, NFATc1, and microphthalmia-associated transcription factor (Mitf) by phosphorylation and dephosphorylation events (Mansky *et al*., 2002; Asagiri and Takayanagi, 2007). RANKL signaling leads to the recruitment of the adaptor molecule TRAF6, followed by the activation and nuclear translocation of NF-κB (Gohda *et al*., 2005; Asagiri and Takayanagi, 2007). When activated, NF-κB triggers c-Fos signals, which then induces nuclear factor of activated T-cells (NFATc1) transcription (Yamashita *et al*., 2007). RANKL signaling also cooperates with costimulatory molecules to trigger calcium influx and turns on calcineurin, which causes activation and nuclear translocation of NFATc1 (Koga *et al*., 2004). After the initial induction, NFATc1 autoamplifies itself through recruitment to its own promoter site, resulting in a selective induction during osteoclast differentiation (Asagiri *et al*., 2005). RANKL activates p38 mitogen-activated protein kinase (MAPK), which in turn phosphorylates Mitf at serine 307 (Mansky *et al*., 2002).

Osteoclast differentiation is regulated by a group of ubiquitous transcription factors that are present in many cell lineages (Thesingh and Scherft, 1985; Grigoriadis *et al*., 1994; Scott *et al*., 1994; Franzoso *et al*., 1997; Iotsova *et al*., 1997; Horsley and Pavlath, 2002; Takayanagi *et al*., 2002; Yamashita *et al*., 2007). The mechanism by which these factors coordinately regulate osteoclast differentiation is poorly understood. Among these transcription factors, Mitf is unique in its tissue-restricted effects. Although present in many tissues, mutations in the *Mitf* gene only profoundly affect certain cell lineages, including osteoclasts, melanocytes, retinal pigmented epithelium, and mast cells (Steingrimsson *et al*., 1994).

Mitf is a basic helix-loop-helix-leucine zipper transcription factor that is able to form homo- and heterodimers with other MiT family members (Tfeb, Tfec, and Tfe3) in vitro (Hemesath *et al*., 1994). Through its basic region, the Mitf dimer binds to the E-box consensus sequence CA[C/T]GTG of target promoters and activates gene transcription. Studies on Mitf in osteoclasts reveal that it transcriptionally regulates the expression of many osteoclast-related genes, including chloride channel 7 (CLCN7), cathepsin K (Ctsk), osteoclast-associated receptor (Oscar), osteopetrosis-associ-

This article was published online ahead of print in *MBoC in Press* (http://www.molbiolcell.org/cgi/doi/10.1091/mbc.E09–07–0584) on March 31, 2010.

Address correspondence to: Yi-Ling Lin (ylin@dentistry.ucla.edu).

Abbreviations used: Ab, antibody; CAII, carbonic anhydrase II; c-Fms, macrophage colony-stimulating factor receptor; mBMM, mouse bone marrow macrophage; CLCN7, chloride channel 7; Ctsk, cathepsin K; CTR, calcitonin receptor; FFPE, formalin-fixed, paraffin-embedded; hPBMC, human peripheral blood mononuclear cell; Mitf, microphthalmia-associated transcription factor; Oscar, osteoclast associated receptor; OPG, osteoprotegrin; ostm1, osteopetrosis-associated transmembrane protein 1; RANK, receptor activator of nuclear factor-κB; RANKL, receptor activator of nuclear factor-κB ligand; semiqRT-PCR, semiquantitative reverse transcriptase-polymerase chain reaction; TRAP, tartrate-resistant acid phosphatase.

ated transmembrane protein 1 (Ostm1), and tartrate resistant acid phosphatase (TRAP) (Luchin *et al.*, 2000; Motyckova *et al.*, 2001; So *et al.*, 2003; Meadows *et al.*, 2007). Interestingly, except for CLCN7, all the Mitf target genes also were reported as transcriptional targets of NFATc1, the osteoclast master transcription factor (Kim *et al.*, 2005; Asagiri and Takayanagi, 2007).

Tfe3 forms stable heterodimers with Mitf in osteoclasts (Weilbaecher *et al.*, 1998). Because Mitf-associated osteopetrosis is observed only with the simultaneous loss of Mitf and Tfe3 in osteoclasts, it is believed that Mitf and Tfe3 are completely redundant in osteoclasts (Steingrimsson *et al.*, 2002). However, recent studies indicated that the relationship between Mitf and Tfe3 may not be as straightforward as once thought, and Tfe3 may not be completely redundant with Mitf in osteoclasts (Sharma *et al.*, 2007).

The *Mitf* gene locus contains at least nine isoform-specific promoters (Steingrimsson *et al.*, 1994; Amae *et al.*, 1998; Fuse *et al.*, 1999; Udono *et al.*, 2000; Oboki *et al.*, 2002; Takeda *et al.*, 2002; Takemoto *et al.*, 2002; Hershey and Fisher, 2005; Shiohara *et al.*, 2008). The consequence of this complex configuration is production of multiple isoforms, which allows the Mitf protein to perform diverse biological functions. Although Mitf is present in many tissues, lineage-specific Mitf isoforms also have been identified in melanocytes (Mitf-M) and mouse mast cells (Mitf-Mc) and are responsible for tissue-specific gene expression (McGill *et al.*, 2002; Takemoto *et al.*, 2002). To date, no osteoclast-specific Mitf isoform has been reported. Both macrophages and osteoclasts are derived from common precursors of the hematopoietic system (Udagawa *et al.*, 1990). Both cells express similar levels of Mitf RNA transcripts (Takayanagi *et al.*, 2002), which raises the question as to how Mitf directs its tissue-specific effect on osteoclasts and whether or not certain isoform(s) is present in osteoclasts but not in macrophages. In this report, we demonstrated that although RANKL has no significant effect on levels of total Mitf and Mitf-A (an abundant and ubiquitously expressed isoform), RANKL significantly up-regulated Mitf-E levels. The goal of this study is to determine whether this induction phenomenon of Mitf isoform has biological significance.

MATERIALS AND METHODS

Materials

α-Ctsk antibody (Ab) was from MBL International (Woburn, MA). α-Hemagglutinin (HA) Ab was from Roche Diagnostics (Mannheim, Germany). α-Tfe3 was from BD Biosciences (San Diego, CA). α-Tubulin Ab was from Sigma-Aldrich (St. Louis, MO). Alexa-conjugated Abs were from Invitrogen (Carlsbad, CA). α-Mitf Ab C5 was a gift from Dr. David E. Fisher (Massachusetts General Hospital, Boston, MA) and also was purchased from Calbiochem (San Diego, CA). Osteoprotegerin (OPG) was purchased from R&D Systems (Minneapolis, MN).

Plasmid Constructs

Mitf isoforms were polymerase chain reaction (PCR)-amplified from mouse osteoclast cDNA and cloned into MSCViG and MSCVpuro (Clontech, Mountain View, CA) plasmids for Mitf-HA and Mitf retrovirus production, respectively. The MSCVpuro plasmid was modified to MSCViG by inserting an IRES-hrGFP fragment with a 5′ HA tag. All constructs were verified by sequencing. Primer information is summarized in Supplemental Table 1.

Isolation of Primary Precursors for Osteoclast and Macrophage Cultures

Long bones were dissected from 2- to 4-mo-old wild-type C57BL/6 mice after euthanasia. Mouse bone marrow was harvested by flushing cold media through the bones with a 22-gauge syringe. All procedures were approved by the Institutional Committee for Animal Care and Use Committee at the University of Kentucky (Lexington, KY). Peripheral blood mononuclear cells (PBMCs) were obtained from buffy coats of healthy human volunteers by Ficoll density gradient centrifugation.

Osteoclast and Macrophage Cultures

For primary osteoclast cultures, precursor cells were cultured in osteoclast media (Osteoclast Precursor Cell Medium Bullet Kit; Lonza Walkersville, Walkersville, MD). For primary macrophage cultures, precursor cells were cultured in the same basal media supplemented only with concentration-matched M-CSF. Media from the primary cultures were replenished every 3 d. RAW264.7 cells were maintained in DMEM and cultured in minimal essential medium (MEM)-α containing various concentrations of RANKL (concentration used is indicated in the figure legends) to induce osteoclastogenesis or in MEM-α without cytokine supplements to maintain macrophage morphology. Media were replenished every 2 d.

Retrovirus Production and Cell Transduction

293 FT cells (Invitrogen) were transfected with retroviral vectors together with pVPack-GP (Stratagene, La Jolla, CA) and pVSV-G (Clontech) by using Lipofectamine 2000 (Invitrogen). Media from the transfected cells were collected and used to infect mouse bone marrow macrophages (mBMMs) or RAW264.7 cells. RAW264.7 Cells transduced with Mitf-HA retroviruses were diluted and plated in 96-well plates with ≤1 cell/well density. Single green fluorescent protein (GFP)-positive plaques were expanded, and expression of the recombinant protein was verified by Western blotting.

RNA Interference and Lentivirus Production

Three lentiviral short hairpin RNAs (shRNAs) targeting the mouse Mitf sequence were purchased from Open Biosystems (Huntsville, AL) (TRCN00000952-84, -86, and -87). Scrambled shRNA with the same vector backbone was purchased from Addgene (Cambridge, MA). To produce lentiviruses, 293 FT cells were transfected with lentiviral vectors and helper plasmids pCMV-DR8.9 and pVSV-G. Media from the transfected cells were collected and used to infect RAW264.7 cells. Infected cells were treated with puromycin (5 μg/ml) for 7 d before culturing in MEM-α containing 100 ng/ml RANKL to induce osteoclast differentiation.

Semiquantitative and Real-Time Reverse Transcriptase (RT)-PCR

Total RNA was isolated from cultured cells with TRIzol reagent (Invitrogen) and from Formalin-fixed, paraffin-embedded (FFPE) tissue samples with High Pure FFPE RNA MicroKit (Roche Applied Science, Indianapolis, IN). For semiquantitative (semiq)RT-PCR, RNA was reverse-transcribed with an oligo(dT) primer to generate cDNA by using a SuperScript First-Strand Synthesis System (Invitrogen). Primer information is summarized in Supplemental Table 1. PCR products were verified by sequencing. Real-time RT-PCR was performed on a LightCycler 2.0 instrument (Roche Applied Science) by using LightCycler RNA Master SYBR Green I according to manufacturer's instructions. LightCycler Probe Design Software 2.0 was used to design the primers. To amplify only mRNA and not genomic DNA, primer sets amplified regions spanning exons were chosen. The specificity of the obtained fluorescence signal was checked by a melting curve analysis after amplification. To exclude the primer–dimer signal, a separate fluorescence detection step (2s) was added after the extension at various temperatures from 79 to 82°C. The relative standard curves of the targets and the reference glyceraldehyde-3-phosphate dehydrogenase (GAPDH) were determined by dilution series of total RNA from RAW264.7-derived osteoclasts. The quantity of the gene was normalized to the quantity of GAPDH, and the data were expressed as fold-induction relative to the calibrator (vector virus infected cells). Experiments were performed on three separate sets of samples and performed in duplicate.

λ Phosphatase Treatment

Cells were lysed in cold buffer (50 mM NaCl, 50 mM Tris-HCl, pH 8.0, 1% NP-40, and Sigmafast Protease Inhibitor [Sigma-Aldrich]), with brief sonication. The lysates were treated with λ phosphatase (New England Biolabs, Ipswich, MA) and incubated at 30°C for 30 min.

Nuclear Extract

RAW264.7 cells were treated with RANKL (100 ng/ml) for 3 d to induce osteoclast differentiation. Cells were first extracted in ice-cold buffer A (10 mM HEPES-KOH, pH 7.9, 1.5 mM $MgCl_2$, 10 mM KCl, 20 mM sodium pyrophosphate, 10 mM NaF, 1 mM Na_3VO_4, and SigmaFAST Protease Inhibitor), incubated on ice for 10 min, and vortexed for 10 s. The lysates were divided into two tubes and centrifuged at 12,000 × *g* for 10 s. The resulting pellets were extracted in two different buffers. One pellet was extracted with ice-cold glycerol/high salt buffer (20 mM HEPES-KOH, pH 7.9, 25% glycerol, 420 mM NaCl, 1.5 mM $MgCl_2$, 0.2 mM EDTA, 20 mM sodium pyrophosphate, 10 mM NaF, 1 mM Na_3VO_4, and SigmaFAST Protease Inhibitor). After a 20-min incubation, the nuclear extract was vortexed for 15 s and spun at 12,000 × *g* at 4°C for 10 min. The other pellet was extracted with SDS/benzonase buffer (2% SDS, 50 mM Tris, pH 6.8, 10% glycerol, 0.1% benzonase

[Sigma-Aldrich], 20 mM sodium pyrophosphate, 10 mM sodium fluoride, 1 mM sodium orthovanadate, and SigmaFAST Protease Inhibitor). The lysates were rotated at room temperature for 15 min to allow benzonase digestion to clarify viscous DNA fragments. Both lysates were cleared by centrifugation, quantified, and analyzed by Western blotting.

Western Blot

Nuclei were lysed with SDS/benzonase buffer or glycerol/high salt buffer as described above, and whole cells were lysed with SDS/benzonase buffer. Proteins were separated on SDS-polyacrylamide gels and transferred to nitrocellulose membranes. Membranes were blocked and incubated with the appropriate primary Ab followed by a horseradish peroxidase-conjugated secondary Ab. The protein signal was developed with enhanced chemiluminescence reagents (Pierce Chemical, Rockford, IL).

Preparation of Bone Discs and Pit Assay

Bovine femurs obtained from local supermarkets were sectioned into 500-μm-thick discs with an EXAKT cutting/grinding system (EXAKT Technologies, Oklahoma City, OK). Osteoclast precursor cells were plated in 24-well dishes containing bone discs in osteoclast media. To assess bone resorption, attached osteoclasts were stripped from the discs by sonication in 0.1 N NaOH. Resorption areas were revealed by staining with 1% toluidine blue in 0.5% sodium tetraborate for 10 min, photographed, and quantified with ImageJ software (National Institutes of Health, Bethesda, MD). The experiments were completed in triplicate.

TRAP Assay

Cells were plated in 24-well plates in triplicate. For the cytochemical assay, cells were fixed and permeabilized with acetone/Formalin/citric acid fixative followed by staining with TRAP solution (kit 387-A; Sigma-Aldrich) at 37°C for 1 h. The cell culture surface corresponding to 37.34 mm^2 was photographed with a 2× objective lens, and ImageJ software was used to quantify the number and the length of the long axis (longest dimension) of multinucleated (>3 nuclei) TRAP-positive cells. For the solution-based TRAP assay, cells were lysed in 1% Triton/phospate-buffered saline before incubation with TRAP solution at 37°C for 1 h. The plates were scanned with a color scanner and the intensity of the positive red color was quantified with ImageJ software. Reactions lacking cells were used as baseline and were subtracted from the scanned results.

Immunofluorescence

mBMMs transduced with Mitf viruses were cultured in the presence of M-CSF and RANKL to induce osteoclast differentiation. Primary osteoclasts were fixed in 2% paraformaldehyde, permeabilized with 0.1% saponin, and blocked with 10% goat serum. Mitf-HA fusion protein was detected by Alexa Fluor 488-conjugated α-HA Ab; Tfe3 was detected by α-Tfe3 Ab with corresponding Alexa Fluor 568-conjugated secondary Ab. Coverslips were mounted with antifade solution containing 4,6-diamidino-2-phenylindole, which stains nuclei. A DM IRBE inverted confocal microscope (Leica Microsystems, Deerfield, IL) was used to acquire images of the nuclei. The colocalization signals of Mitf and Tfe3 in the nuclear sections were quantified by ImageJ software using JACoP plugin. The colocalization images were generated by ImageJ software using Colocalization Highlighter plugin.

Statistical Analysis

Data were analyzed using an unpaired two-tailed Student's *t* test and were expressed as mean ± SD; $p \leq 0.05$ is considered significant.

RESULTS

Mitf-E Is Differentially Expressed in Macrophages and Osteoclasts, and Its Expression Is Induced by RANKL

To determine whether any of the currently identified Mitf isoforms are differentially expressed in macrophages and osteoclasts, the expression profiles of Mitf isoforms of both cell types were compared. To eliminate interspecies differences, human (h) PBMCs, mBMMs, and the mouse macrophage cell line RAW264.7 were used to generate the cultures. Osteoclast differentiation was verified by TRAP staining and bone resorption on bovine bone discs. Multinucleated TRAP+ cells were present in all three osteoclast cultures (Supplemental Figure 1). Both RAW264.7 cells and mBMMs cultured under macrophage conditions were mononuclear and TRAP-negative. Human macrophages were TRAP-positive but mostly mononuclear, although freshly isolated human monocytes were TRAP-negative (data not shown). All three osteoclast cultures produced resorption areas as evidenced by the pit formation on bovine bone discs (Supplemental Figure 1).

Total RNA derived from verified cultures was subjected to semiqRT-PCR by using isoform-specific 5′ primers for Mitf, paired with a common 3′ primer. GAPDH was measured as a loading control, whereas total Mitf, amplified by primer pairs flanking common regions of Mitf transcripts, was amplified to ensure that Mitf was expressed in all RNA samples. Previous studies with RAW264.7 cells showed that total Mitf expression did not change significantly after RANKL treatment (Takayanagi *et al*., 2002). However, when we examined the individual Mitf isoforms, Mitf-E signal was significantly up-regulated in all three osteoclast cultures (Figure 1A). This universal induction in osteoclasts, in comparison with macrophages, seemed to be caused by RANKL stimulation and was uniquely found for Mitf-E, because no other isoforms examined exhibited similar consistent induction or suppression in all three culture systems. Mitf-A was the most abundant isoform in both cell types and represented the major signal detected in total Mitf, but its expression levels were unchanged for both macrophages and osteoclasts (Figure 1A). Mitfs B, C, D, and H were present in low amounts, and the transcripts could only be detected after 35 cycles. Mitf J was present in moderate quantities and, depending on the cell source, was detectable between 29 and 35 cycles. Finally, Mitf-M (melanocytes) and Mitf-Mc (mast cells) are tissue specific and were therefore not detected at all in macrophages or osteoclasts. To date, human Mitf-Mc and mouse Mitf CM have not yet been described.

Archived human biopsy tissues were used for investigating Mitf expression in vivo. Tissue blocks with diagnoses of giant cell granuloma or nonspecific chronic inflammation were identified from the Axium database at the University of Kentucky. Giant cell granuloma is characterized by the presence of multinucleated giant cells that are osteoclasts in nature (Bonetti *et al*., 1990; Itonaga *et al*., 2002; Itonaga *et al*., 2003). Nonspecific chronic inflammation is granulation tissue consisting of a composite of chronic inflammatory cells, including many mononuclear macrophages. Sections were obtained for total RNA extraction followed by RT-PCR with primers specific for Mitf-A, Mitf-E, and total Mitf. M-CSF receptor c-fms and CD68 are macrophage markers and were used as loading controls. Figure 1B shows that Mitf-E was present in giant cell granuloma but could not be detected in nonspecific inflammatory tissue despite the presence of similar levels of Mitf-A and macrophage markers in both lesions.

When ectopically expressed in 293 FT cells (Figure 1C), Mitf-E cannot be differentiated from other smaller isoforms based on the electrophoretic mobility, whereas Mitf-A, which is ubiquitously expressed and abundantly present in macrophages and osteoclasts, migrated as higher bands from the smaller isoforms. Mitf proteins were represented by multiple bands, reflecting the presence of multiple isoforms and a consequence of posttranslational modification (Figure 1C). Western blot analysis showed that Mitf proteins, as expected from the RT-PCR results in Figure 1A, were differentially expressed between RAW264.7 cells treated with or without RANKL for osteoclast differentiation (Figure 1D, lanes 1 and 2). The induced Mitf proteins were noted in RAW264.7 cells treated with RANKL and were smaller in molecular weight than Mitf-A, although indistinguishable from other Mitf isoforms, including Mitf-E. In RAW264.7 cells received no RANKL treatment, low amounts of Mitf proteins smaller than Mitf-A also were noted and were likely low level-expressing Mitf isoforms.

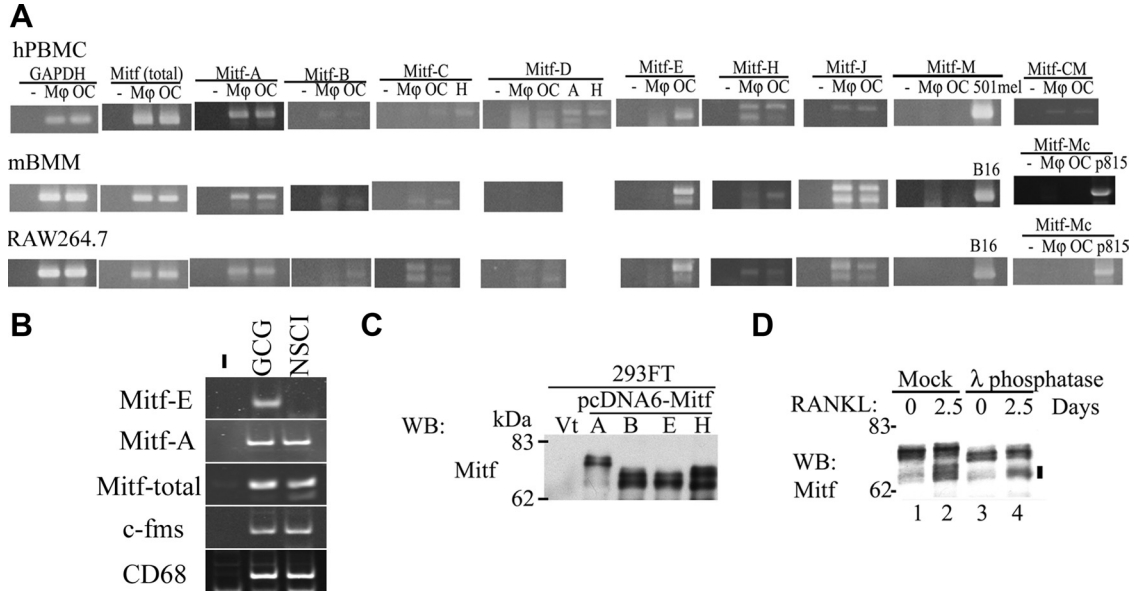

Figure 1. Mitf-E is differentially expressed in macrophages and osteoclasts. (A) semiqRT-PCR of Mitf isoforms. cDNA was isolated from macrophages and osteoclasts derived from hPBMCs, mBMMs, and RAW264.7 cells. H (HeLa), A (APRE19), 501mel, B16, and p815 cells were used as positive controls for PCR. Mitf exhibits internal exon splicing, which contributes to the presence of multiple bands in some of the gels. −, no cDNA; Mφ, macrophage; OC, osteoclast. (B) semiqRT-PCR of Mitf signals in giant cell granuloma (GCG) and nonspecific chronically inflamed tissue (NSCI). (C) Western blot of ectopically expressed Mitf isoforms in 293 FT cells. (D). Western blots of lysates from RAW264.7 cells treated with or without RANKL. The lysates were subjected to phosphatase or mock treatment before blotting with α-Mitf Ab. Vertical bar, RANKL-induced Mitf.

In addition to the induction of the smaller Mitf proteins, osteoclast differentiation of RAW264.7 by RANKL treatment also resulted in additional upper bands in Mitf-A region (Figure 1D, lanes 2 vs. 1). To verify that these upper bands were caused by RANKL-induced phosphorylation of Mitf-A and not by induction of unidentified Mitf isoforms, we treated the RAW264.7 lysates with λ phosphatase. When compared with mock treated lysates, λ phosphatase treatment not only caused a collapse of the Mitf-A upper band in the lysate of RANKL-treated cells (Figure 1D, lane 4 vs. 2), but also dephosphorylated Mitf-A from cells with or without RANKL treatment to similar electrophoretic mobilities (Figure 1D, lanes 3 and 4). λ phosphatase also caused an upper band collapse of RANKL-induced Mitf protein (Figure 1D, lane 4 vs. 2, marked by vertical bar). These results indicated that phosphorylated Mitf-A was present in RAW264.7 cells, and RANKL treatment not only induced and phosphorylated RANKL-induced Mitf protein but also resulted in additional phosphorylation of Mitf-A.

Because Mitf-E induction during osteoclastogenesis seemed to be caused by RANKL stimulation, the kinetics of this process were examined. RAW264.7 cells cultured in the presence of RANKL were harvested at various time points for semiqRT-PCR and Western blot analysis. The results showed that Mitf-E mRNA levels were induced by RANKL within 6–12 h, peaked at 24 h, and then declined by 48 h (Figure 2A, left). After 48 h, fresh media containing RANKL was added to restimulate a new round of Mitf-E induction. Mitf-E mRNA repeaked within 12 h (60 h after initial RANKL stimulation) followed by a gradual decline. Most of the RANKL in the culture media was consumed by the cells in 2 to 3 d as there was no reinduction on day 3 when the media was not replenished with fresh RANKL (Supplemental Figure 2). Osteoprotegerin (OPG), a RANKL decoy receptor and specific inhibitor, was used to verify whether the Mitf-E induction is indeed caused by RANKL or by other proteins present in the RANKL recombinant protein preparation. The results showed that when OPG was added in the presence of RANKL, it disrupted RANKL signals, which abolished Mitf-E induction (Figure 2A, right). Together, these results showed that RANKL signaling specifically induces Mitf-E expression. Figure 2B shows that RANKL-induced Mitf protein (marked by vertical bar) followed similar kinetics as the Mitf-E mRNA.

Although the RANKL-induced Mitf bands may be caused by multiple isoforms including those that have not yet been identified, based on the induction levels observed in the RT-PCR results and the similarity of the induction kinetics of Mitf-E mRNA and RANKL-induced protein, Mitf-E seems to contribute significantly to the RANKL-induced Mitf pro-

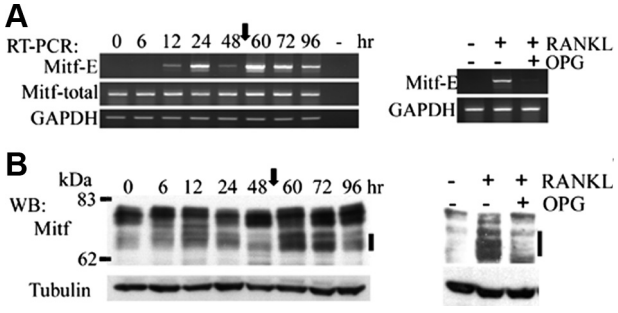

Figure 2. RANKL regulates Mitf-E expression. RAW264.7 cells were incubated with 100 ng/ml RANKL. The arrows indicate times during which the media were changed. (A) semiqRT-PCR. Left, time course of Mitf-E levels after RANKL treatment. Right, addition of OPG abolishes Mitf-E induction by RANKL. GAPDH serves as a cDNA loading control. (B) Western blot. Left, Time course of RANKL-induced Mitf protein (marked by vertical bar). Right, addition of OPG abolishes RANKL-induced Mitf expression. α-Tubulin is a protein loading control.

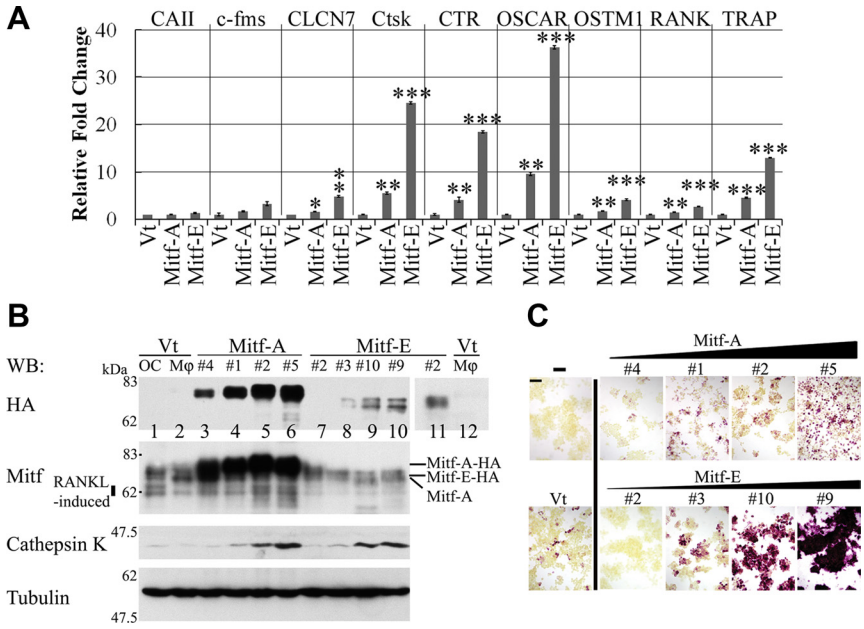

Figure 3. Mitf-E is a more potent osteoclastogenic factor than Mitf-A. (A) Real-time PCR of osteoclast-related genes in RAW264.7-derived osteoclasts transduced with Mitf-A or Mitf-E retrovirus. Student's *t* test: *p ≤ 0.01, **p ≤ 0.005, and ***p ≤ 0.001. (B) Western blots of RAW264.7 clones expressing various levels of Mitf-A or Mitf-E HA fusion proteins. α-Tubulin is a loading control. Vector-transduced RAW264.7 cells were cultured with or without RANKL (50 ng/ml) for macrophage (Mφ) or osteoclast (OC) cultures, respectively. Vertical bar, RANKL-induced Mitf. #, designated clone number of RAW264.7 clones. (C) TRAP stain of RAW264.7 clones transduced with Mitf retroviruses. Cells were cultured in the absence of RANKL. Bar, 50 μm.

teins. Together, these data provide convincing evidence that Mitf-E is specifically induced by RANKL and differentially expressed between macrophages and osteoclasts.

Mitf-E Is a More Potent Osteoclastogenic Factor Than Mitf-A

To examine the effects of Mitf proteins on genes involved in osteoclast function, we infected RAW264.7 cells with Mitf-A-HA-, Mitf-E-HA-, or vector (null)-expressing retroviruses, and then we treated the cells with RANKL to induce osteoclast differentiation. Expression levels of various osteoclast-related genes were determined by real-time RT-PCR. These genes included carbonic anhydrase II (CAII), macrophage colony-stimulating factor receptor (c-Fms), CLCN7, Ctsk, calcitonin receptor (CTR), Oscar, Ostm1, receptor activator of NF-κB (RANK), and TRAP. CLCN7, TRAP, Ctsk, Oscar, and Ostm1 were identified previously as Mitf targets (Luchin *et al.*, 2000; Motyckova *et al.*, 2001; So *et al.*, 2003; Meadows *et al.*, 2007). TRAP, Ctsk, and Oscar were identified as targets by overexpressing Mitf-M, whereas CLCN7 and Ostm1 were identified by overexpressing Mitf-A. The results showed that Mitf-A and Mitf-E up-regulated most of

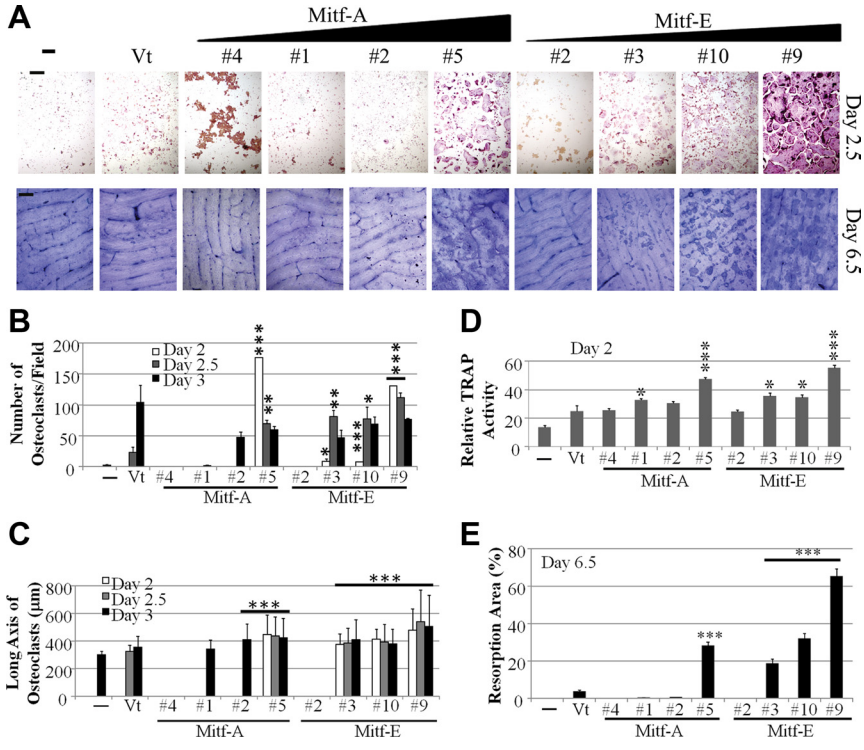

Figure 4. Mitf-A and Mitf-E have different osteoclastogenic activities. RAW264.7 clones expressing Mitf-HA were plated on culture dishes and on bovine bone discs in media containing 50 ng/ml RANKL to induce osteoclast differentiation. (A) Top, TRAP stain. Bar, 500 μm. Bottom, toluidine blue stain of resorption areas. Bar, 200 μm. (B) Quantitation of numbers of multinucleated TRAP-positive cells. Only p values of day 2 and 2.5 cultures were determined. (C) Quantitation of sizes of multinucleated TRAP+ cells. (D) Quantitation of TRAP activity. (E) Quantitation of bone resorption areas. The data are expressed as mean ± SD, n = 3 except for C. The sample number of C is the sum of multinucleated TRAP+ cells from three photographed fields. n = 6–528. Student's *t* test: *p ≤ 0.01, **p ≤ 0.005, and ***p ≤ 0.001. Cells transduced by vector-expressing viruses were used as control for p value calculations. Only cells ≥250 μm were counted in B and C.

the genes examined except CAII (Figure 3A). In addition to the five previously identified target genes, both Mitf isoforms also up-regulated CTR and RANK despite the induction levels of RANK were low compared with other targets. Mitf-E also mildly up-regulated c-Fms in certain cases; however, this stimulatory effect could not be consistently reproduced. Interestingly, expression of Mitf-E results in higher levels of the majority of these osteoclast-related genes than Mitf-A.

To further examine the roles of Mitf-A and Mitf-E in osteoclastogenesis, multiple independent Mitf clones were generated from transduced RAW264.7 cells. Four representative clones from each group were selected for analysis to characterize the differences between the two isoforms. The expression of recombinant and total Mitf proteins were analyzed by blotting with α-HA and α-Mitf Abs, respectively (Figure 3B). The clones were arranged in ascending order corresponding to recombinant Mitf expression levels. Mitf-E clone #2 (Figure 3B, first panel, lanes 7 and 11) expressed very low amounts of recombinant protein, detectable only after a substantially long exposure of the blot to x-ray film. The Mitf-A clones expressed recombinant Mitf-A protein levels well above the endogenous Mitf-A levels (Figure 3B, second panel, lanes 3–6 vs. 1–2). The recombinant Mitf-E protein migrated with a similar electrophoretic mobility as endogenous Mitf-A due to the presence of the HA epitope, thus making it difficult to accurately estimate its expression level in the clones. However, Mitf-E clones had recombinant protein levels not exceeding above the levels of endogenous RANKL-induced Mitf proteins (Figure 3B, second panel, lanes 7–10 vs. 1, marked by vertical bar).

Real-time RT-PCR (Figure 3A) showed that expression of Mitf-A and Mitf-E significantly up-regulated Ctsk and TRAP transcripts in RAW264.7 cells treated with RANKL. When we examined whether or not the up-regulation of these genes was RANKL-dependent, Western blot results showed that both Mitf-A and Mitf-E could induce Ctsk expression independent of RANKL treatment (Figure 3B, third panel). Despite being expressed at much lower levels, recombinant Mitf-E was able to promote Ctsk expression to levels comparable with recombinant Mitf-A. The expression of TRAP, an osteoclast marker, also was examined in clones cultured without RANKL, the result of which showed that both Mitf-A and Mitf-E were able to induce TRAP expression independent of RANKL treatment (Figure 3C). In this case, despite being expressed at much lower levels, recombinant Mitf-E was able to promote TRAP expression much more than Mitf-A. Therefore, Mitf-E has a greater ability than Mitf-A in activating Ctsk and TRAP expressions regardless of RANKL treatment.

To assess whether Mitf-E is more proficient than Mitf-A in promoting osteoclast differentiation, we examined the ability of the previously generated Mitf-transduced clones to undergo osteoclast differentiation by plating cells in the presence of RANKL. Osteoclastogenesis was determined by counting the number of multinucleated TRAP+ cells in the cultures and by evaluating the abilities of the cells to resorb bone (Figure 4). As expected, both Mitf-A and Mitf-E stimulated osteoclast differentiation. However, the levels of Mitf required for detectable stimulating effects were strikingly different between the two isoforms. Among the Mitf-E clones, all except for clone 2 (the lowest Mitf-E expression) exhibited accelerated osteoclastogenesis corresponding with an overall increase in numbers of osteoclasts, TRAP expression, cell sizes and bone resorption (Figure 4). In the Mitf-A group of clones, although expressing high levels of Mitf, only clone #5 (the highest Mitf-A expression) displayed significant stimulatory results. These results demonstrate that Mitf-E has significantly higher osteoclastogenic activity than Mitf-A.

Mitf-A and Mitf-E Have Different Subnuclear Distribution

Both Mitf-A and Mitf-E share all known functional domains, except for an extended amino terminus of additional 52 amino acids present in Mitf-A. We investigated whether the two isoforms exhibited a different subnuclear localization. Mouse primary osteoclasts transduced with Mitf-HA viruses were stained with HA and Tfe3 Abs, and confocal microscopy was used to scan the nuclei. The HA and Tfe3 colocalization nuclear images were generated by Colocalization Highlighter and the Pearson's coefficient was quantified by JACoP (Bolte and Cordelieres, 2006). The results showed that Mitf-A protein exhibited a more diffuse signal, whereas the Mitf-E signal was much more discrete in the nuclei of osteoclasts (Figure 5A). The pattern differences were subtle but distinctive. The presence of overexpressed Mitf proteins apparently affected the distribution of the endogenous bind-

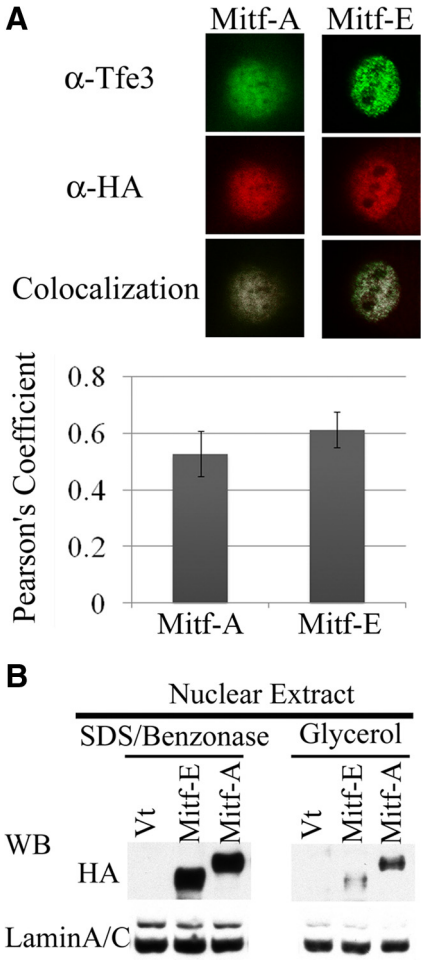

Figure 5. Mitf-A and Mitf-E have a different subnuclear distribution. (A) Top, confocal nuclear images of mouse osteoclasts transduced with Mitf-A-HA or Mitf-E-HA retroviruses. The cells were stained with α-HA and α-Tfe3 Abs. Bottom, correlation coefficient of Tfe3 and Mitf signals. (B) Differential extraction with different buffer conditions on RAW264.7-derived osteoclasts transduced with Mitf retroviruses. Nuclear lysates extracted by SDS/benzonase or glycerol/high salt buffer were blotted with α-HA and α-Lamin A/C Abs. α-Lamin A/C serves as a loading control.

ing partner Tfe3. The colocalization images of Mitf and Tfe3 proteins highlighted the differences of the two isoforms. Mitf-E also showed a slightly higher colocalization correlation with Tfe3 than Mitf-A in the nuclei. Although the differences were mild, they were very consistent.

We also used a biochemical approach to examine the two isoforms' subnuclear distribution. RAW264.7 cells were transduced by Mitf-HA viruses and RANKL was used to induce osteoclast differentiation. The nuclei of the osteoclasts were extracted into two different buffers and the extractability of Mitf-A versus Mitf-E was examined. The cells were sequentially extracted, first with a hypotonic buffer to remove cytoplasmic proteins, followed by nuclear extraction with either glycerol/high salt without detergent or SDS/benzonase buffer. The results showed that although nuclear extraction with the glycerol/high salt buffer yielded high amounts of Mitf-A and low amounts of Mitf-E in the lysates, extraction with the SDS/benzonase buffer resulted in equally high amounts of Mitf-A and Mitf-E (Figure 5B).

These findings suggest that Mitf-A and Mitf-E have a different subnuclear distribution. The majority of Mitf-A is probably present in a compartment that is readily to be extracted by high salt buffers, whereas removal of chromatin, either by benzonase digestion (Figure 5B) or by sonication shearing (Figure 1D), facilitates Mitf-E extraction.

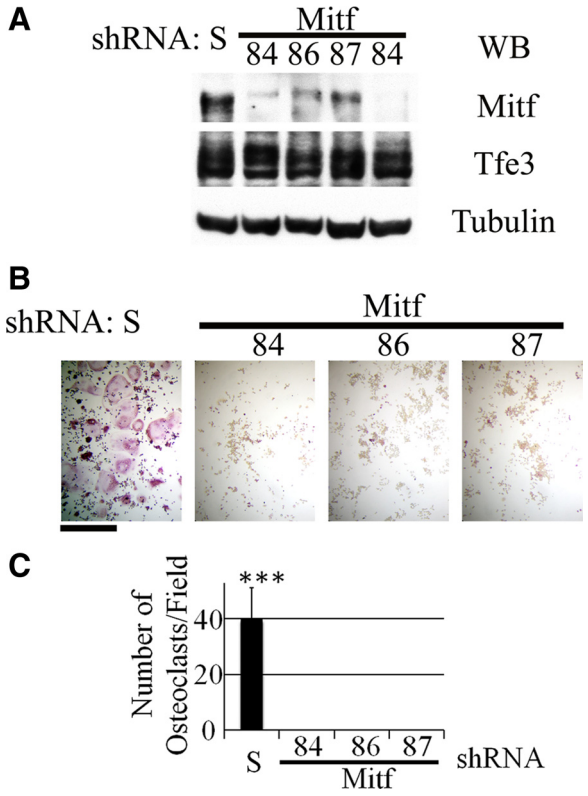

Figure 6. Reducing Mitf expression inhibits osteoclastogenesis in vitro. (A) Western blot analyses of lysates from RAW264.7 cells infected by lentiviruses expressing Mitf or scrambled (S) shRNA. α-Tubulin serves as a loading control. (B) TRAP staining of infected cells cultured in media containing 100 ng/ml RANKL for 3 d. (C) Quantitation of multinucleated TRAP-positive cells in (B). Bar, 500 μm. Student's t test: ***$p \leq 0.001$.

Mitf Is Essential for Osteoclast Differentiation In Vitro, but Expression of Mitf-A Alone Is Insufficient to Fully Support Osteoclastogenesis in Mitf Knockdown RAW264.7 Cells

Mitf is critical for osteoclast development, as evidenced by the lack of osteoclasts in osteopetrotic Mitf$^{mi/mi}$ mice. Although the current theory supports Mitf-Tfe3 redundancy in osteoclast development (Steingrimsson *et al.*, 2002), there are research findings challenging this concept (Sharma *et al.*, 2007). To examine whether Mitf is indispensable in osteoclast differentiation, shRNA lentiviruses targeting three different regions of Mitf transcripts were used to infect RAW264.7 preosteoclast cells. All three Mitf shRNAs, but not the scrambled shRNA, specifically knocked down Mitf expression in the cells but did not affect Tfe3 expression (Figure 6A). Correspondingly, all three Mitf shRNAs significantly inhibited osteoclastogenesis when infected cells were cultured in the presence of RANKL to induce osteoclast differentiation. (Figure 6, B and C). These data provide the first evidence that although there seems to be functional redundancy between Mitf and Tfe3 in vivo, Tfe3 is unable to fully compensate for the absence of Mitf during osteoclastogenesis in vitro.

It is important to ask whether the induction of Mitf-E, in the presence of ample amounts of Mitf-A, has biological significance to osteoclastogenesis. We examined whether expressing either isoform similarly to endogenous levels was sufficient to rescue osteoclastogenesis in RAW264.7 cells in which Mitf expression was silenced by RNA interference. shRNA-Mitf84 targets the 3′-untranslated region that is present only in the endogenous Mitf transcripts; therefore, it has no suppressive effect on the recombinant Mitf molecules. The cells transduced with lentivirus expressing shRNA-Mitf84 were cultured with RANKL to induce osteoclast differentiation. As expected, shRNA-Mitf84 significantly knocked down Mitf expression (Figure 7A, lane 5). As well, no oste-

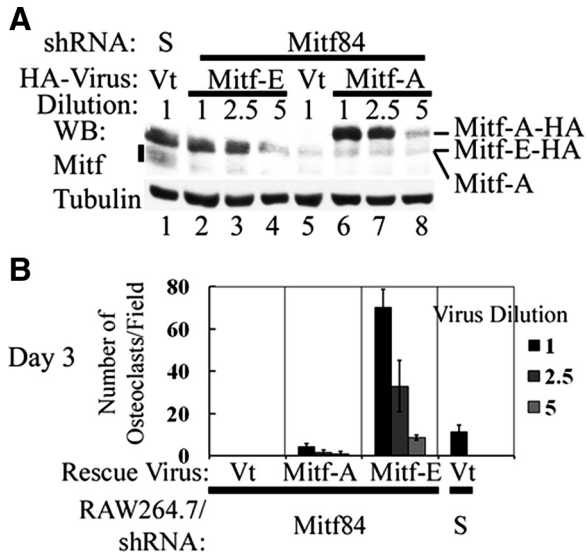

Figure 7. Mitf-A and Mitf-E rescue osteoclastogenesis with different efficacies in Mitf knockdown RAW264.7 cells. (A) Western blot analysis of Mitf expression. Cells were transduced by Mitf or scrambled shRNA lentiviruses followed by rescue with vector (Vt)- or Mitf-expressing viruses diluted 1, 2.5, or 5 times. Vertical bar, RANKL-induced Mitf. (B) Quantitation of multinucleated TRAP+ cells. The cells were cultured in media containing 100 ng/ml RANKL for 3 d.

oclasts were identified in the cultures when the cells were infected with virus carrying the vector alone (Figure 7B). In contrast, expression of either recombinant Mitf-A– or Mitf-E–mediated osteoclastogenesis, although with different efficacy of rescue. Mitf-A–expressing viruses, when diluted 1 and 2.5 times before infecting cells, produced more recombinant protein than endogenous Mitf-A, but when diluted 5 times, resulted in less recombinant protein made. (Figure 7A, lanes 6–8 vs. 1). With every dilution, the expression of recombinant Mitf-A resulted in partial rescue of osteoclastogenesis (Figure 7B), indicating that activated Mitf-A alone, when expressed close to the endogenous levels, is insufficient to support full-scale operation of osteoclastogenesis. Recombinant Mitf-E, due to its HA epitope, has a similar electrophoretic mobility as endogenous Mitf-A. This made accurate assessment of the recombinant protein levels somewhat difficult. Nonetheless, it was clear that when the viruses were diluted 5 times, the resulting recombinant Mitf-E expression did not exceed endogenous RANKL-induced protein levels (Figure 7A, lane 4 vs. 1, marked by vertical bar). In contrast to the results of Mitf-A, at this dilution of the Mitf-E-expressing virus, osteoclastogenesis was restored to nearly the same extent of the control cells (Figure 7B), indicating the functional potency and importance of Mitf-E for osteoclastogenesis.

DISCUSSION

During osteoclastogenesis, Mitf is presumably activated by phosphorylation induced by RANKL signaling pathway (Mansky *et al*., 2002). Our data showed that RANKL not only triggers phosphorylation but also induces expression of Mitf proteins. In this study, Mitf-E was the only known isoform examined that was RANKL-inducible and seemed to be a stronger osteoclastogenic factor than the ubiquitously expressed Mitf-A. Although it is necessary to silence Mitf-E specifically to conclude its role in osteoclastogenesis, the induction phenomenon of Mitf proteins seems to be important because our results suggest that activation of Mitf-A alone is insufficient to support osteoclastogenesis. Mitf-A, despite its abundant presence, seems to be a weak osteoclastogenic factor and requires assistance from other isoforms, such as Mitf-E, to support osteoclastogenesis.

Unlike Mitf-A, Mitf-E is not ubiquitously expressed in normal tissues. Mouse mast cells, except peritoneal mast cells, are the other cell type that expresses significant levels of Mitf-E (Oboki *et al*., 2002). Structurally, Mitf-E is a truncated version of Mitf-A and is 90% identical to Mitf-A. Both isoforms share all known functional domains in the downstream protein-coding sequence, common to all the Mitf isoforms. It is unexpected that their effects on osteoclastogenesis are so drastically different. Based on the results of differential extractions, we propose a model that Mitf-E is induced during osteoclasotgenesis, and this isoform is in close association with chromatin, which facilitates its interaction with target promoters. This may be the underlying mechanism for Mitf-E's higher osteoclastogenic activity than Mitf-A.

Tfe3 forms heterodimers with Mitf in osteoclasts (Weilbaecher *et al*., 1998), and studies of $Tfe3^{fcr/fcr}$ knockout and $Mitf^{vga9/vga9}$ transgenic mice have led to the conclusion that Mitf and Tfe3 are completely redundant (Steingrimsson *et al*., 2002). This is because both mutant mice have a normal bone phenotype, and only mice manifesting $Mitf^{vga9/vga9}Tfe3^{fcr/fcr}$ double mutations become severely osteopetrotic (Steingrimsson *et al*., 2002). However, $Mitf^{vga9}$ is not a null allele. It was generated by a transgene insertion at the *mi* locus, which disrupted the expression of Mitf-M and caused a significant reduction of overall Mitf expression (Tachibana *et al*., 1992; Hodgkinson *et al*., 1993). A recent study by Sharma *et al*. (2007) provided some evidence that the relationship between Mitf and Tfe3 may be more complicated than was proposed previously. They noted that 38.8% $Mitf^{mi/vga9}$ compound heterozygous mice were osteopetrotic, whereas both $Mitf^{mi+}$ and $Mitf^{vga/+}$ mice have a normal bone phenotype. The mutation in the $Mitf^{mi}$ allele results in Mitf proteins that have lost their capacity to bind DNA but yet retain the ability to form dimers with Tfe3 (Steingrimsson *et al*., 1994). Therefore, acting as dominant negatives, $Mitf^{mi}$ mutant proteins disrupt the Mitf–Tfe3 pathway. The authors pointed out that $Mitf^{mi/vga9}$ compound heterozygous mice would not have been osteopetrotic if Mitf and Tfe3 were completely redundant (Sharma *et al*., 2007), because the only difference between the $Mitf^{mi/vga9}$ and $Mitf^{mi/+}$ mice is that the $Mitf^{mi/vga9}$ mice have a lower levels of wild-type Mitf proteins than $Mitf^{mi/+}$ mice. Interestingly, our RNA interference results suggest that Tfe3's role during in vitro osteoclastogenesis is limited. Our data provide the first evidence that although there seems to be functional redundancy between Mitf and Tfe3 in vivo, Tfe3 is unable to fully compensate for the absence of Mitf during osteoclastogenesis in vitro. The underlying cause for the difference in results could be attributed to osteoclast progenitors receiving additional signals from other cell types in the developmental environment versus an experimental condition whereby pure osteoclast cells are used such as in the in vitro culture milieu. Although this hypothesis remains to be tested, it is obvious that Mitf and Tfe3 have distinct roles and are not completely redundant during osteoclastogenesis.

In this report, we showed that Mitf proteins are critical for osteoclastogenesis. This is evidenced by their ability to upregulate several osteoclast-related genes in the presence or absence of RANKL and their indispensability during osteoclastogenesis in vitro. The discoveries that Mitf isoforms are regulated differentially by RANKL and activated Mitf-A alone is insufficient to account for the osteoclastogenic activities in the cells suggest that the RANKL-induced Mitf phenomenon may play a pivotal role during osteoclastogenesis. The induction of Mitf-E by RANKL may be a critical event to coordinate with other ubiquitously expressed transcription factors for osteoclastogenesis.

ACKNOWLEDGMENTS

We thank Dr. David E. Fisher for the α-Mitf Ab (C5) and Dr. Clifford Takemoto for p815 cells. We also thank Drs. Rina Plattner, Marnie M. Saunders, and Jeffery L. Ebersole for critical reading of the manuscript. This study was supported by National Center for Research Resources grant P20 RR15592 and National Institute of Dental and Craniofacial Research grant R03 DE019490 (to Y.L.L.).

REFERENCES

Amae, S., *et al*. (1998). Identification of a novel isoform of microphthalmia-associated transcription factor that is enriched in retinal pigment epithelium. Biochem. Biophys. Res. Commun. *247*, 710–715.

Asagiri, M., *et al*. (2005). Autoamplification of NFATc1 expression determines its essential role in bone homeostasis. J. Exp. Med. *202*, 1261–1269.

Asagiri, M., and Takayanagi, H. (2007). The molecular understanding of osteoclast differentiation. Bone *40*, 251–264.

Bolte, S., and Cordelieres, F. P. (2006). A guided tour into subcellular colocalization analysis in light microscopy. J. Microsc. *224*, 213–232.

Bonetti, F., Pelosi, G., Martignoni, G., Mombello, A., Zamboni, G., Pea, M., Scarpa, A., and Chilosi, M. (1990). Peripheral giant cell granuloma: evidence for osteoclastic differentiation. Oral Surg. Oral Med. Oral Pathol. *70*, 471–475.

Franzoso, G., Carlson, L., Xing, L., Poljak, L., Shores, E. W., Brown, K. D., Leonardi, A., Tran, T., Boyce, B. F., and Siebenlist, U. (1997). Requirement for NF-kappaB in osteoclast and B-cell development. Genes Dev. *11*, 3482–3496.

Fuse, N., *et al*. (1999). Molecular cloning of cDNA encoding a novel microphthalmia-associated transcription factor isoform with a distinct amino-terminus. J. Biochem. *126*, 1043–1051.

Gohda, J., Akiyama, T., Koga, T., Takayanagi, H., Tanaka, S., and Inoue, J. (2005). RANK-mediated amplification of TRAF6 signaling leads to NFATc1 induction during osteoclastogenesis. EMBO J. *24*, 790–799.

Grigoriadis, A. E., Wang, Z. Q., Cecchini, M. G., Hofstetter, W., Felix, R., Fleisch, H. A., and Wagner, E. F. (1994). c-Fos: a key regulator of osteoclast-macrophage lineage determination and bone remodeling. Science *266*, 443–448.

Hemesath, T. J., Steingrimsson, E., McGill, G., Hansen, M. J., Vaught, J., Hodgkinson, C. A., Arnheiter, H., Copeland, N. G., Jenkins, N. A., and Fisher, D. E. (1994). Microphthalmia, a critical factor in melanocyte development, defines a discrete transcription factor family. Genes Dev. *8*, 2770–2780.

Hershey, C. L., and Fisher, D. E. (2005). Genomic analysis of the Microphthalmia locus and identification of the MITF-J/Mitf-J isoform. Gene *347*, 73–82.

Hodgkinson, C. A., Moore, K. J., Nakayama, A., Steingrimsson, E., Copeland, N. G., Jenkins, N. A., and Arnheiter, H. (1993). Mutations at the mouse microphthalmia locus are associated with defects in a gene encoding a novel basic-helix-loop-helix-zipper protein. Cell *74*, 395–404.

Horsley, V., and Pavlath, G. K. (2002). NFAT: ubiquitous regulator of cell differentiation and adaptation. J. Cell Biol. *156*, 771–774.

Iotsova, V., Caamano, J., Loy, J., Yang, Y., Lewin, A., and Bravo, R. (1997). Osteopetrosis in mice lacking NF-kappaB1 and NF-kappaB2. Nat. Med. *3*, 1285–1289.

Itonaga, I., Hussein, I., Kudo, O., Sabokbar, A., Watt-Smith, S., Ferguson, D., and Athanasou, N. A. (2003). Cellular mechanisms of osteoclast formation and lacunar resorption in giant cell granuloma of the jaw. J. Oral Pathol. Med. *32*, 224–231.

Itonaga, I., Schulze, E., Burge, P. D., Gibbons, C. L., Ferguson, D., and Athanasou, N. A. (2002). Phenotypic characterization of mononuclear and multinucleated cells of giant cell reparative granuloma of small bones. J. Pathol. *198*, 30–36.

Kim, Y., Sato, K., Asagiri, M., Morita, I., Soma, K., and Takayanagi, H. (2005). Contribution of nuclear factor of activated T cells c1 to the transcriptional control of immunoreceptor osteoclast-associated receptor but not triggering receptor expressed by myeloid cells-2 during osteoclastogenesis. J. Biol. Chem. *280*, 32905–32913.

Koga, T., *et al*. (2004). Costimulatory signals mediated by the ITAM motif cooperate with RANKL for bone homeostasis. Nature *428*, 758–763.

Lagasse, E., and Weissman, I. L. (1997). Enforced expression of Bcl-2 in monocytes rescues macrophages and partially reverses osteopetrosis in op/op mice. Cell *89*, 1021–1031.

Luchin, A., Purdom, G., Murphy, K., Clark, M. Y., Angel, N., Cassady, A. I., Hume, D. A., and Ostrowski, M. C. (2000). The microphthalmia transcription factor regulates expression of the tartrate-resistant acid phosphatase gene during terminal differentiation of osteoclasts. J. Bone Miner. Res. *15*, 451–460.

Mansky, K. C., Sankar, U., Han, J., and Ostrowski, M. C. (2002). Microphthalmia transcription factor is a target of the p38 MAPK pathway in response to receptor activator of NF-kappa B ligand signaling. J. Biol. Chem. *277*, 11077–11083.

McGill, G. G., *et al*. (2002). Bcl2 regulation by the melanocyte master regulator Mitf modulates lineage survival and melanoma cell viability. Cell *109*, 707–718.

Meadows, N. A., Sharma, S. M., Faulkner, G. J., Ostrowski, M. C., Hume, D. A., and Cassady, A. I. (2007). The expression of clcn7 and ostm1 in osteoclasts is coregulated by microphthalmia transcription factor. J. Biol. Chem. *282*, 1891–1904.

Motyckova, G., Weilbaecher, K. N., Horstmann, M., Rieman, D. J., Fisher, D. Z., and Fisher, D. E. (2001). Linking osteopetrosis and pycnodysostosis: regulation of cathepsin K expression by the microphthalmia transcription factor family. Proc. Natl. Acad. Sci. USA *98*, 5798–5803.

Oboki, K., Morii, E., Kataoka, T. R., Jippo, T., and Kitamura, Y. (2002). Isoforms of mi transcription factor preferentially expressed in cultured mast cells of mice. Biochem. Biophys. Res. Commun. *290*, 1250–1254.

Scott, E. W., Simon, M. C., Anastasi, J., and Singh, H. (1994). Requirement of transcription factor PU. 1 in the development of multiple hematopoietic lineages. Science *265*, 1573–1577.

Sharma, S. M., Bronisz, A., Hu, R., Patel, K., Mansky, K. C., Sif, S., and Ostrowski, M. C. (2007). MITF and PU. 1 recruit p38 MAPK and NFATc1 to target genes during osteoclast differentiation. J. Biol. Chem. *282*, 15921–15929.

Shiohara, M., Shigemura, T., Suzuki, T., Tanaka, M., Morii, E., Ohtsu, H., Shibahara, S., and Koike, K. (2008). MITF-CM, a newly identified isoform of microphthalmia-associated transcription factor, is expressed in cultured mast cells. Int. J. Lab. Hematol. *31*, 215–226.

So, H., Rho, J., Jeong, D., Park, R., Fisher, D. E., Ostrowski, M. C., Choi, Y., and Kim, N. (2003). Microphthalmia transcription factor and PU.1 synergistically induce the leukocyte receptor osteoclast-associated receptor gene expression. J. Biol. Chem. *278*, 24209–24216.

Steingrimsson, E., *et al*. (1994). Molecular basis of mouse microphthalmia (mi) mutations helps explain their developmental and phenotypic consequences. Nat. Genet. *8*, 256–263.

Steingrimsson, E., Tessarollo, L., Pathak, B., Hou, L., Arnheiter, H., Copeland, N. G., and Jenkins, N. A. (2002). Mitf and Tfe3, two members of the Mitf-Tfe family of bHLH-Zip transcription factors, have important but functionally redundant roles in osteoclast development. Proc. Natl. Acad. Sci. USA *99*, 4477–4482.

Tachibana, M., Hara, Y., Vyas, D., Hodgkinson, C., Fex, J., Grundfast, K., and Arnheiter, H. (1992). Cochlear disorder associated with melanocyte anomaly in mice with transgenic insertional mutation. Mol. Cell. Neurosci. *3*, 433–445.

Takayanagi, H., *et al*. (2002). Induction and activation of the transcription factor NFATc1 (NFAT2) integrate RANKL signaling in terminal differentiation of osteoclasts. Dev. Cell *3*, 889–901.

Takeda, K., Yasumoto, K., Kawaguchi, N., Udono, T., Watanabe, K., Saito, H., Takahashi, K., Noda, M., and Shibahara, S. (2002). Mitf-D, a newly identified isoform, expressed in the retinal pigment epithelium and monocyte-lineage cells affected by Mitf mutations. Biochim. Biophys. Acta *1574*, 15–23.

Takemoto, C. M., Yoon, Y. J., and Fisher, D. E. (2002). The identification and functional characterization of a novel mast cell isoform of the microphthalmia-associated transcription factor. J. Biol. Chem. *277*, 30244–30252.

Thesingh, C. W., and Scherft, J. P. (1985). Fusion disability of embryonic osteoclast precursor cells and macrophages in the microphthalmic osteopetrotic mouse. Bone *6*, 43–52.

Udagawa, N., Takahashi, N., Akatsu, T., Tanaka, H., Sasaki, T., Nishihara, T., Koga, T., Martin, T. J., and Suda, T. (1990). Origin of osteoclasts: mature monocytes and macrophages are capable of differentiating into osteoclasts under a suitable microenvironment prepared by bone marrow-derived stromal cells. Proc. Natl. Acad. Sci. USA *87*, 7260–7264.

Udono, T., *et al*. (2000). Structural organization of the human microphthalmia-associated transcription factor gene containing four alternative promoters. Biochim. Biophys. Acta *1491*, 205–219.

Weilbaecher, K. N., Hershey, C. L., Takemoto, C. M., Horstmann, M. A., Hemesath, T. J., Tashjian, A. H., and Fisher, D. E. (1998). Age-resolving osteopetrosis: a rat model implicating microphthalmia and the related transcription factor TFE3. J. Exp. Med. *187*, 775–785.

Yamashita, T., *et al*. (2007). NF-kappaB p50 and p52 regulate receptor activator of NF-kappaB ligand (RANKL) and tumor necrosis factor-induced osteoclast precursor differentiation by activating c-Fos and NFATc1. J. Biol. Chem. *282*, 18245–18253.